

Supplementary Material to “Magnetospheric “magic” frequencies as magnetopause surface eigenmodes”

M. O. Archer, M. D. Hartinger, T. S. Horbury

Geophysical Research Letters (2013GL057908)

With the criteria used in selecting events in this study, the possibility of events overlapping one another exists hence there could potentially be bias in the results if a majority of events overlapped. Indeed, magnetosheath jets are known to be quasiperiodic often recurring on timescales of a few minutes, though there are often periods of the order of an hour or more when jets do not occur [e.g. *Archer et al.*, 2012]. The distribution (number per hour) of selected magnetosheath jets in time is shown in Figure 1(top) for both the high and low f_{FLR} cases.

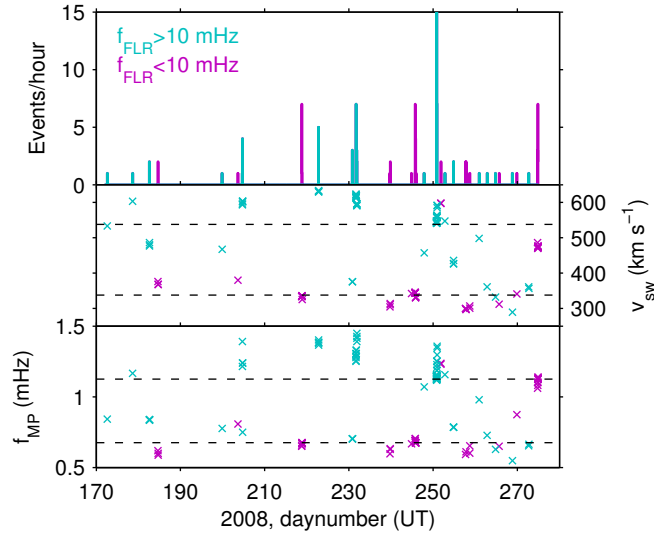


Figure 1: (top) Distribution of selected magnetosheath jet events in time, displaying the number of events per hour for the high (turquoise) and low (purple) FLR frequency cases. (middle & bottom) Solar wind speed (middle) and estimated fundamental magnetopause surface eigenfrequency (bottom) for each event for both FLR frequency cases (colors as before).

It is clear that in the $f_{FLR} < 10$ mHz case, events are fairly spread out over a number of different days with typically only 1 or 2 events per hour and only three cases of 5 events per hour. Therefore, we are confident that the results presented in the paper are reliable and not biased by any particular day. On the other hand, in the $f_{FLR} > 10$ mHz case there is one quite dominant day (day 250 i.e. 6 September 2008) with up to 15 events per hour. In fact 30% of the $f_{FLR} > 10$ mHz events come from this day. Therefore, it is likely this particular day biases the calculated median spectra. Therefore, we recalculated these (both the power spectral densities and wavelet transforms) for all $f_{FLR} > 10$ mHz events but excluding those from day 250 as well as those only for day 250.

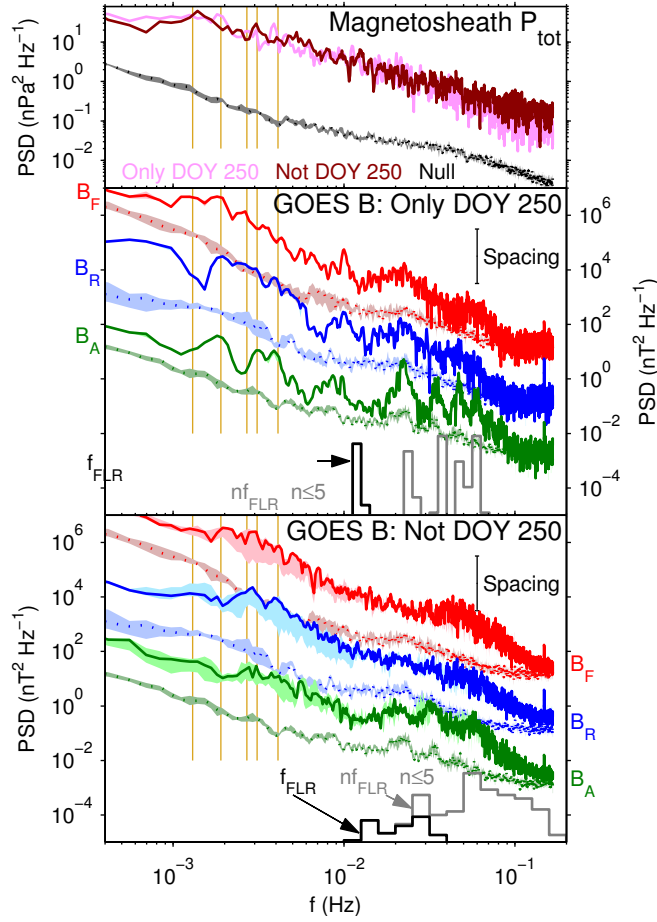


Figure 2: Median power spectra of the magnetosheath total pressure (top) and magnetospheric magnetic field components (middle & bottom) for the high FLR frequency events only on day 250 (middle) and excluding day 250 (bottom) in the same format as Figure 2a of the paper.

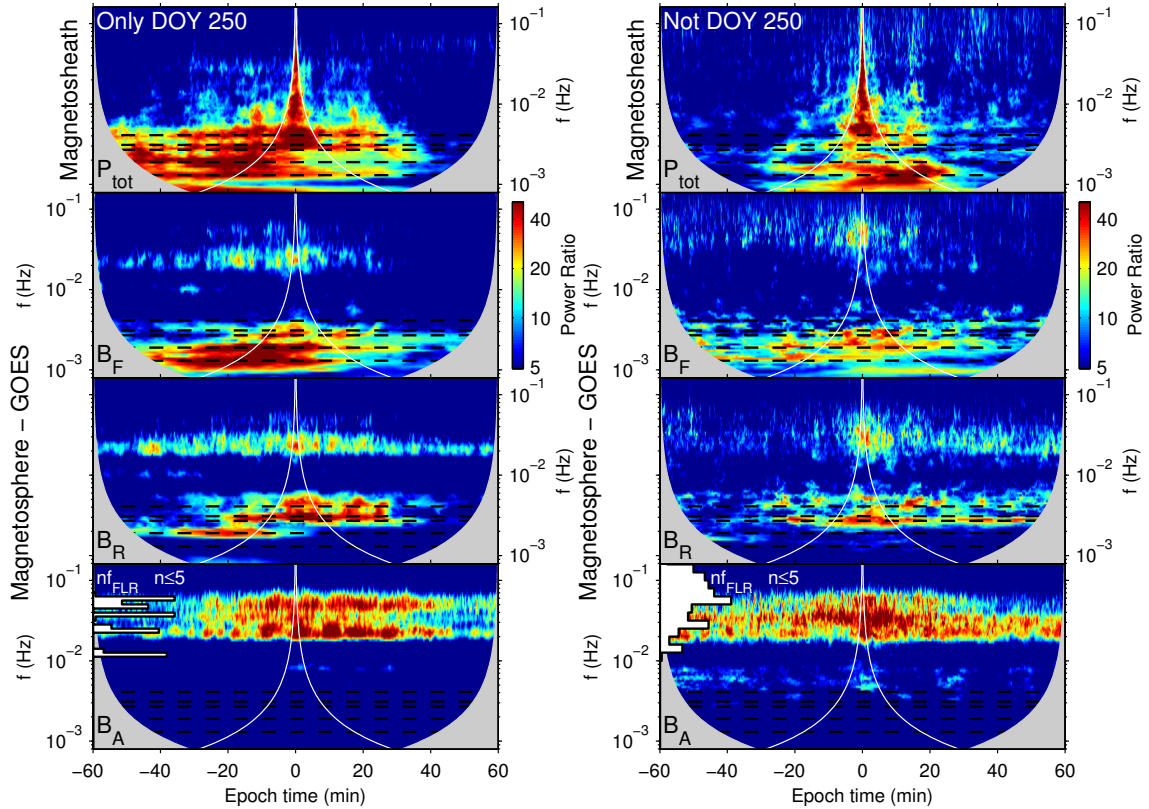


Figure 3: Median dynamic spectra for the high FLR frequency events on day 250 only (left) and excluding day 250 (right) in the same format as Figure 2b of the paper.

Figure 2 shows the median power spectra for both these cases. It is clear that the power spectra of day 250 highly resemble the results of the paper and thus the median spectra are to a certain extent biased by this day. However, the results excluding day 250 are qualitatively similar to those presented in the paper. The power spectral densities showed enhancements in the toroidal component at the most common FLR frequency harmonics (grey histogram in bottom panel of Figure 2) as well as at some of the “magic” frequencies. The latter were clearest (and most significant) in the poloidal component, with smaller enhancements in both the compressional and toroidal components.

Figure 3 shows the median dynamic spectra for both cases also. While the results for day 250 show some clear differences to those in the paper, particularly in the driving magnetosheath pressure before the jets, the median dynamic spectra excluding day 250 showed many of the same features as those presented: broadband driving, power enhancements at low and typically “magic” frequencies and slight changes in the spectral response before and after the jet. Therefore, the overall results of the paper remain.

Figure 1 also shows the solar wind speed (middle) and estimated magnetopause eigenfrequencies f_{MP} (bottom) for all events. It is clear that events in slow (fast) wind correspond to low (high) f_{MP} and occurred on a number of days. Therefore the correlation between these quantities presented in the paper is not simply due to two populations of events at similar times.

The distributions of conditions (solar wind and the Dst index) over all events as well as for the high f_{FLR} case (and the null events) are shown in Figure 4, demonstrating the wide range mentioned in the paper. These surprisingly resulted in preferential “magic” frequencies. Larger statistical studies could address how such preferential frequencies arise from the distributions of solar wind properties and compare the predicted magnetopause surface eigenfrequencies with observations of magnetic pulsations.

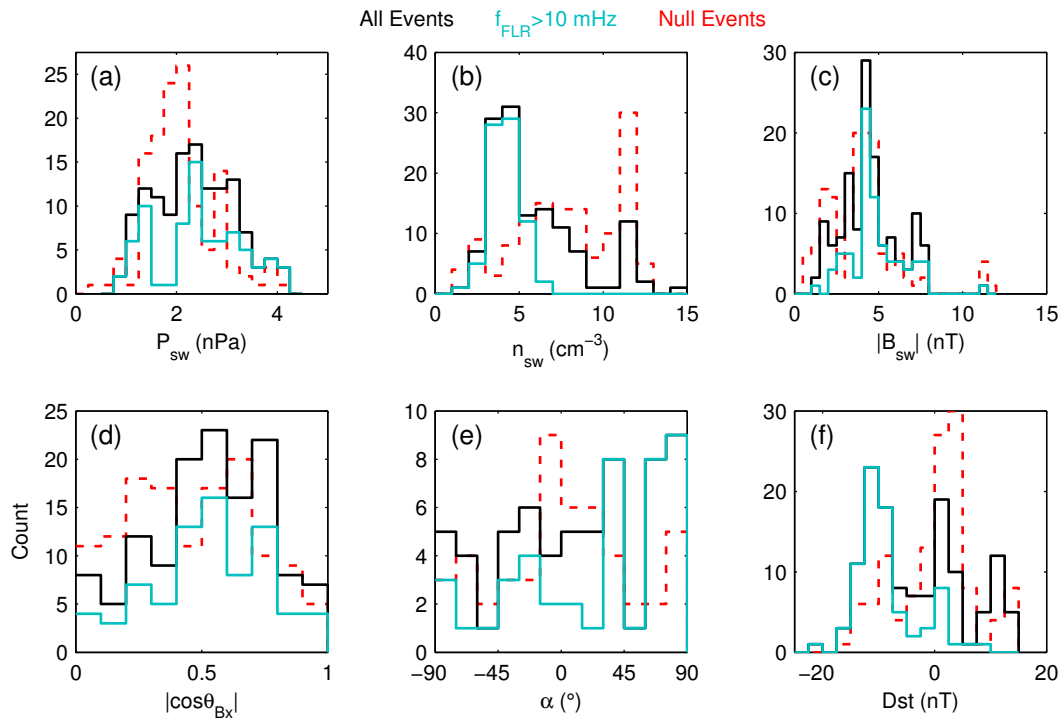


Figure 4: Distributions of conditions for all events (black), high FLR frequency events (turquoise) and the null events (red) showing solar wind dynamic pressure (a), density (b), interplanetary magnetic field (IMF) magnitude (c), IMF cone angle (d), IMF clock angle (e), and the disturbance storm time index (f).

References

Archer, M. O., T. S. Horbury, and J. P. Eastwood, Magnetosheath pressure pulses: generation downstream of the bow shock from solar wind discontinuities, *J. Geophys. Res.*, *117*, A05,228, doi:10.1029/2011JA017468, 2012.